ELSEVIER

Journal of Nuclear Materials 313–316 (2003) 478–490

journal of nuclear materials

www.elsevier.com/locate/jnucmat

# Tritium retention of plasma facing components in tokamaks

T. Tanabe [a,*], N. Bekris [b], P. Coad [c], C.H. Skinner [d], M. Glugla [b], N. Miya [e]

[a] *Center for Integrated Research in Science and Engineering, Nagoya University, Chikusa-ku, Furo-cho, Nagoya 464-8603, Japan*
[b] *Tritium Laboratory, Forschungszentrum, Karlsruhe, P.O. Box 3640, 76021, Germany*
[c] *EURATOM/UKAEA Fusion Association, Culham Science Centre, Culham, Abingdon Oxon, OX14 3DB, UK*
[d] *Princeton Plasma Physics Laboratory, Princeton, NJ 08543, USA*
[e] *Japan Atomic Energy Research Institute, Naka Fusion Research Establishment, 801 Mukouyama, Naka-machi, Naka-gun, Ibaraki-ken 311-0193, Japan*

**Abstract**

The areal distribution of tritium retention in tiles from TEXTOR, TFTR, JT-60U and JET has been measured via the imaging plate technique and the results are discussed from the perspective of carbon–hydrogen chemistry. It is found that the observed tritium distribution clearly shows asymmetries in poloidal and toroidal directions and also reflects the local temperature history of the analyzed tiles. We show the first clear evidence of the loss of high energy tritons by toroidal magnetic field ripple. We distinguish three different contributions to tritium retention in tokamaks with carbon plasma facing components: high energy tritons escaping from the core plasma, low energy ions and neutrals from the edge plasma, and molecular tritium from gas fueling. These components are retained at different depths and with different concentrations. Tritium from the edge plasma dominates the retained inventory but could be reduced if the surface temperature was higher. We propose tokamak operation with plasma facing components above 1000 K as a possible way to reduce the tritium inventory.


*PACS:* 52.40.H
*Keywords:* Tritium; Inventory; Retention mechanism; TEXTOR; JT-60U; TFTR; JET; Divertor; First wall

## 1. Introduction

Tritium retention is a critical issue facing next step magnetic fusion devices with carbon plasma facing components [1–3]. Experience in JET and TFTR showed tritium retention of 40% and 51% respectively during plasma operations. After several weeks of cleanup (D-operation, $D_2$ and He-glow, $O_2$-venting) about 12% and 16% of the tritium remained as long term tritium retention [4–6]. Modeling predicts that the in-vessel tritium limit of ITER could be reached in the order of 100 pulses [7–9]. Fast and efficient tritium removal is necessary for the proposed schedule of plasma operations. Detritiation by a scanning laser has shown promise [10] but no suitable tritiumu removal has yet bee adequately demonstrated in a tokamak.

In JET and TFTR, tritium distributions have been measured employing a technique combining combustion with liquid scintillation [11–13] and also by tile baking and an open wall ion chamber [5,14]. Fig. 1 shows the tritium surface concentration in MBq/cm$^2$ of a poloidal set of JET Mark IIA divertor tiles [11]. Most of the tritium was retained in the low temperature area of the divertor, particularly in shadowed regions at the inner divertor and louvers in front of cryopumps. However, these measurements are time consuming and the spatial resolution is limited.

In a D–T reactor, the energy of tritium impinging onto the wall must be widely distributed, because tritium

* Corresponding author. Tel.: +81-52 789 5157; fax: +81-52 789 5177/5158/3225.
*E-mail address:* tanabe@cirse.nagoya-u.ac.jp (T. Tanabe).

0022-3115/03/$ - see front matter 
PII: S0022-3115(02)01377-6

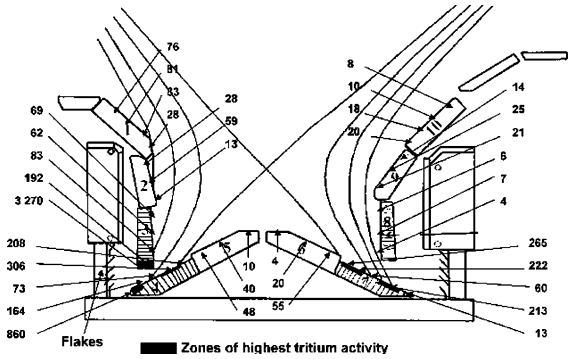


Fig. 1. Cross-section of the Mark IIA divertor in JET. All tiles except 5 and 6 were analyzed by the IP technique. The numbers are the tritium surface concentration within 1 mm from the surface in MBq/cm$^2$ measured by the coring/combustion technique [11–13].

is introduced by either gas puffing, NBI injection or pellet injection. In addition, the D–D reaction in the plasma produces 1 MeV tritons. This suggests that even in the present tokamaks, tritium distribution should be quite dependent on fueling techniques and geometry. The tritium distribution should also be dependent on wall temperature but no systematic investigations have been made.

Quite recently, we have successfully applied the tritium imaging plate (IP) technique [15] to determine the surface tritium distribution on plasma facing tiles. This is an autoradiography technique relying on the beta particles produced by tritium decay. The betas have a range of about several micrometers in graphite and hence the technique is sensitive to tritium in the depth of a few microns. A Fuji imaging plate (BAS-TR20250) was placed in contact with the tiles for a duration of hours to days (depending on the tritium level) and the surface tritium distribution was subsequently read out by the generation of photo-stimulated luminescence (PSL) in an imaging plate reader with 100 μm transverse spatial resolution. For highly activated tiles, a polyphenylene sulfide (PPS) film of 2–10 μm thickness was placed between the imaging plate and the tile to prevent contamination of the plate reader. Gamma radiation could be discriminated against by separating the tile and imaging plate with a thick film that transmitted only the gammas.

We have measured the tritium spatial distribution on various graphite tiles taken from TEXTOR [15–17], TFTR, JT-60U [18–21] and JET [22]. It is found that the observed tritium distribution clearly shows asymmetries in poloidal and toroidal directions and also reflects the local temperature history of the analyzed tiles. It is also noted that toroidal tritium distribution in JT-60U clearly shows the ripple loss due to toroidal field inhomogeneity[16]. In addition, the profile of deuterium (D) and hydrogen (H) is sometimes quite different from that of tritium (T) [17].

These findings motivate us to compare the tritium retention behavior in different tokamaks and to a make systematic analysis based on the present knowledge for carbon–hydrogen chemistry. From this analysis we conclude that if a D–T reactor is operated at a higher temperature than that of the present tokamak, the tritium inventory can be greatly reduced. The paper is organized as follows: firstly carbon–hydrogen chemistry is briefly reviewed and the characteristics of tritium impinging the plasma facing tiles in a carbon based D–T reactor is identified. Then we summarize the results of our tritium retention studies by the imaging plate technique in large tokamaks, focusing on the toroidal and poloidal non-uniform tritium distribution that were clearly observed by IP technique for the first time. Taking all these into account, we discuss tritium retention in D–T reactors, particularly from the aspect of inventory reduction We propose to maintain plasma facing surface temperature at about 1000 K during plasma operations in order to reduce the tritium inventory in carbon based plasma facing components.

## 2. Carbon–hydrogen chemistry

Carbon–hydrogen system has been extensively studied because of its importance for the practical use of amorphous hydrogenated carbon (a:C–H), or diamond like carbon films, which are grown by plasma assisted or thermal decompositions (co-deposition) of various gas phase hydrocarbons. However, the multiple bonding nature of elemental carbon, (i.e., sp, sp$^2$ and sp$^3$ hybridization) makes the characterization of a:C–H films as well as the hydrogen implanted graphite, very complicated. Jacob and Moeller [23] have characterized various a:C–H films by the amount of sp$^2$ and sp$^3$ carbon and hydrogen as shown in Fig. 2. The sp

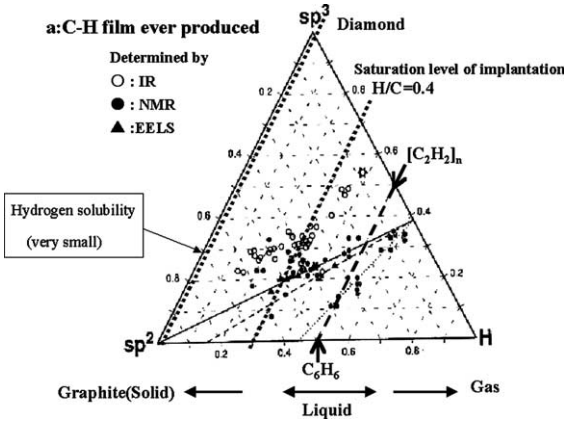


Fig. 2. Composition of a:C–H films [23].

hybridization is neglected due to its low abundance. Generally, higher hydrogen content leads to soft carbon films, while lower hydrogen content leads to hard diamond-like carbon films. In hydrogen-saturated carbon films made by hydrogen ion irradiation at incident energies above a few 10's of eV, the maximum H/C ratio is known to be around 0.4 [24–27]. Deposition from a low temperature plasma ($\ll$10 eV) sometimes gives softer film with higher hydrogen content of H/C around $\approx$1 [28]. However, such film may not be stable under high heat load. To remain as a solid phase, the hydrogen content must be less than the $H/C = 1$ line on the axis of H-$sp^3$ axis (i.e., $[C_2H_2]_n$ or poly-ethylene) and on the H-$sp^2$ axis (i.e., $C_6H_6$ or benzene). Higher H/C ratios lead to liquid and gas phases. In general, as illustrated in Fig. 2, the H/C ratio in an a:C–H film is limited to certain range depending on the production methods and deposition temperature. According to thermodynamics, graphite and diamond are not miscible (or soluble) with each other. Hence carbon atoms with different characteristics such a $sp^2$ and $sp^3$ hybridization are believed to be mixed as shown in Fig. 2. However a quite recent report has suggested the existence of some intermediate state between $sp^2$ and $sp^3$ [29]. Thus, until now no one has succeeded in determining the 'tie lines' usually drawn in such a phase diagram to indicate the solubility limit and co-existing phases.

The phase diagram is strongly temperature dependent. As shown in Fig. 3 [30], the saturated hydrogen concentration decreases with increasing temperature and becomes very small at $T > 1000$ K. Below 500 K, graphite irradiated with hydrogen ions until saturation reportedly shows the same characteristics as that of hydrogen-saturated a:C–H films [26,27]. With increasing substrate temperature, the H/C ratio in the deposited film decreases, and the film becomes poly-crystalline graphite or pyrolytic carbon, partially but not fully graphitized carbon. It should also be mentioned that thermal desorption of implanted hydrogen is quite concentration dependent, that is, the lower the concentration, the higher the desorption temperature [25,27]. Graphite is believed to absorb hydrogen exothermically. However, the very small solubility (ppm level) and diffusivity make the determination of true solubility difficult, as will be discussed in the next section.

Radiation damage of graphite enhances apparent hydrogen solubility as shown in Fig. 4 [31]. Retained hydrogen is chemically bonded to a carbon atom in a:C–H films and in hydrogen-saturated graphite. The very low solubility of hydrogen in graphite indicates that only bonded C–H can stay in the a:C–H film during the co-deposition process, that is dangling bonds in the solid phase produced by energetic particle injection can trap hydrogen and create a chemical bond. This explains the increase of the apparent hydrogen solubility by damage production in graphite, e.g., the neutron irradiated graphite showing a larger apparent solubility than the non-irradiated ones in Fig. 4 [31]. Interestingly, the apparent hydrogen solubility is also found to be a simple function of the degree of graphitization, a measure for the completeness of the microstructure of graphite, in both irradiated or non-irradiated graphite [31,35].

Diffusion in graphite crystals is also very small. However, because of the porous structure (even 'high density nuclear graphite' only has about 80% of the theoretical density of a perfect crystal), gaseous hydrogen can permeate through graphite very rapidly (migration through pores). This means that every grain in the graphite plate is simultaneously exposed to a gaseous atmosphere with only a small static pressure gradient. In addition, migration through pores also makes the release of methane and hydrogen molecules possible within

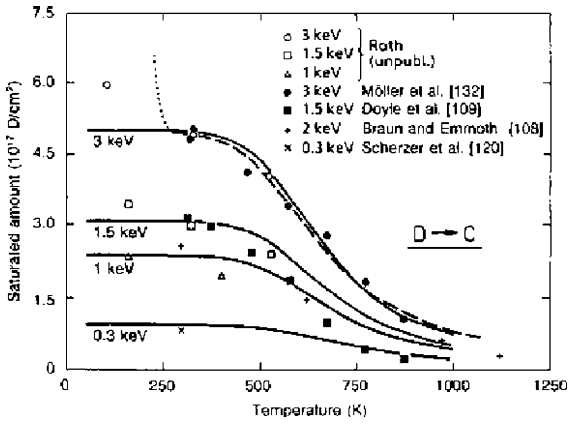


Fig. 3. Temperature dependence of hydrogen saturation level for various graphite implanted with hydrogen ions after Doyle et al. [30].

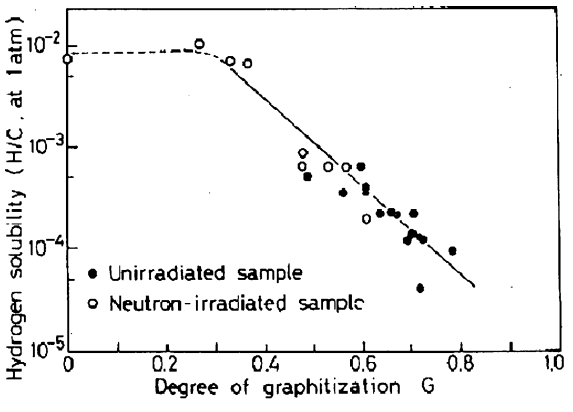


Fig. 4. Dependence of hydrogen solubility on degree of graphtization. Closed circles are for nuclear graphites and open circles are for neutron irradiated ones [31].

graphite during hydrogen ion irradiation. See reviews [3,25,27] and references therein for detailed hydrogen migration mechanism.

## 3. Tritium in fusion reactors

### 3.1. Source of tritium

In D–T burning tokamak reactors, one can distinguish four different tritium sources; (i) the 'edge plasma tritium' directly impinging from the boundary plasma, with an energy of a few eV to several hundreds of eV [32], (ii) the 'high energy tritium' produced from the D–D nuclear reaction in the plasma, (iii) 'gaseous tritium' puffed in to the vessel but which did not fuel the plasma and was evacuated through pump ducts, and (iv) tritium produced in structure materials by nuclear transmutation, which is not discussed here. The edge plasma tritium will be, of course, the main source of tritium retention in plasma facing walls in future burning plasmas. The high energy tritium is the only tritium source in present D–D discharge devices. It is important to note that tritium produced by D–D reaction has an initial energy of 1 MeV and is likely to impinge into the plasma facing surface before complete thermalization to the plasma temperature. A recent simulation shows around 30% of produced tritium could be implanted without fully loosing its initial energy through rippleloss mechanism even in a DT reactor [33]. Actually, the toroidal tritium distribution in JT-60U clearly shows the ripple loss due to toroidal field inhomogeneity [34]. Although the cross-section for D–D reaction is less than 1/10 of that for the D–T reaction, tritium produced by the D–D reaction (around 1/200–1/500 of the produced neutron amount in a D–T reactor) [33] might be a serious concern, because it can reach deeper regions in the plasma facing materials and is difficult to remove compared to the tritium adsorbed or co-deposited on the surface. In fact, tritium retention in deeper regions than hydrogen and deuterium was confirmed in graphite tiles used in TEXTOR [15–17] and JT-60U [18–21]. The retention of the gaseous tritium was clearly observed in JET tiles, as will be shown in later sections. The contribution of the gaseous tritium retention in one graphite tile was very small, but the integrated amount from back sides of all PFM tiles could contribute significantly to the total tritium retention.

### 3.2. Tritium retention mechanisms

Fig. 5 shows the schematics of hydrogen retention in plasma facing tiles [35]. Because of the porous nature of graphite, the depth profiles of retained hydrogen originating from energetic hydrogen and molecular hydrogen are quite different, i.e. energetic hydrogen impinges directly into surface layers and stops at around its projected range, whereas molecular hydrogen can penetrate deeply along open pores (see Section 2). As a result, gaseous hydrogen can penetrate deeply or permeate through a graphite plate. However, the very small diffusivity inhibits hydrogen migration into the grains. Therefore, macroscopic depth profiles exhibit smooth changes (see side illustrations in Fig. 5) even if the detailed or microscaled profiles in each grain is significantly different.

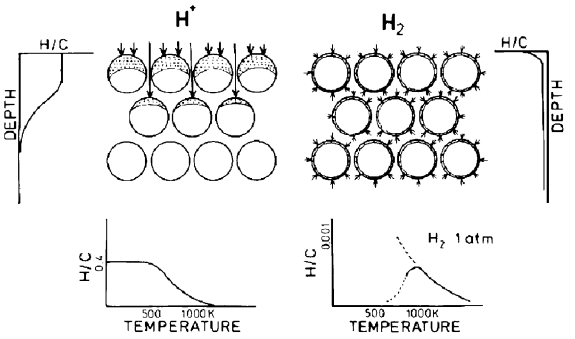


Fig. 5. Simplified model given by Tanabe [35] for the surface retention by energetic hydrogen injection from plasma and the bulk retention due to residual gass in a trous.

In addition, hydrogen retention in graphite is very temperature dependent. Below 500 K, the implanted hydrogen is trapped and immobile, and the surface region is quickly saturated with an H/C ratio of about 0.4 for H/C for incident ion energies above a few 10's of eV. Above 800 K, hydrogen diffusion becomes dominant and above 1000 K most of the implanted hydrogen recombines at the grain surface and is re-emitted through open pores. Atomic hydrogen release also begins above 1300 K. Because of the exothermic nature of hydrogen solubility, in general, the temperature dependence of retention of gaseous hydrogen must be similar to that of the ion implanted hydrogen. However, retention measurements with gaseous hydrogen show a temperature dependence as shown in the dotted line given in the bottom right of Fig. 5, i.e., with increasing temperature the apparent retention increases (the increase of diffusivity overcomes the reducing solubility) showing a maximum at around 1000 K and then decreases owing to the exothermic nature of hydrogen solubility shown as the dashed line in the figure. Once hydrogen molecules are formed on the grain surface by a bulk re-combination mechanism [26,27] (mobile atomic hydrogen re-combining with trapped hydrogen), hydrogen molecules can migrate to the top surface and be released.

It should be noted that the temperature range where the implanted hydrogen concentration changes rapidly is around 500–800 K. As will be discussed, the temperature of plasma facing surfaces sometimes passes this

temperature range during a discharge, which is clearly seen in the tritium retention behavior in JT-60U. This may be the cause of difficulties in density control with hydrogen saturated graphite walls in small tokamaks. In JET [36] and JT-60U [37] the first wall is operated at around 600 K and the divertor tiles in JET were very likely below 550 K because they were fixed at the water-cooled base plates and heated mainly by radiation), while TFTR tiles were at room temperature but some plasma facing surface increased to $\leqslant 1000$ K in high power discharges [5,38]. Other significant differences (maybe more significant for erosion behavior) are the edge temperature (100's of eV in TFTR, less than 10 eV in JET divertor) producing either physical or chemical sputtering, the magnetic field geometry, and scrape-off layer flows. These remain for future investigation.

## 4. Tritium in D–D discharge machines (high energy tritium)

### *4.1. Tritium retention in plasma facing graphite tiles from TEXTOR*

Fig. 6 compares the photograph and the tritium image of one of the ALT-II limiter tiles from TEXTOR [15,16]. As seen in the line profiles in Fig. 6(a), the tritium distribution in the erosion-dominated region is nearly uniform and much higher than that in the deposition-dominated region. The measured tritium level at the erosion-dominated was about 100 Bq/cm$^2$ [39]. This is nearly the same level as the tritium level calculated by assuming that all tritium produced is uniformly implanted into the plasma facing surface. This indicates that the implantation of the high energy tritons into the plasma facing surfaces is the main mechanism. By peeling off some area of the deposited layer (indicated in the upper left region of the tritium image in Fig. 6(a)), the tritium level beneath the deposited layer was again uniformly distributed with the tritium levels somewhat higher than that of the erosion-dominated region.

It is interesting to compare the tritium profile with deuterium and boron profiles measured by the ion beam analysis [40] of one of the ALT-II tiles; see Fig. 6(b) [17,40]. As clearly seen in Fig. 6(b), deuterium and boron show quite similar profiles and their densities are higher at the re-deposition dominated region (poloidal position $>80$ mm). In other words, deuterium was retained in a very shallow region by re- or co-deposition with boron and carbon, whereas tritium was retained deeper [34].

Fig. 7(a) and (b) show the photographs and the corresponding tritium images of the top and the bottom tiles from 5 TEXTOR bumper limiter tiles. The toroidal

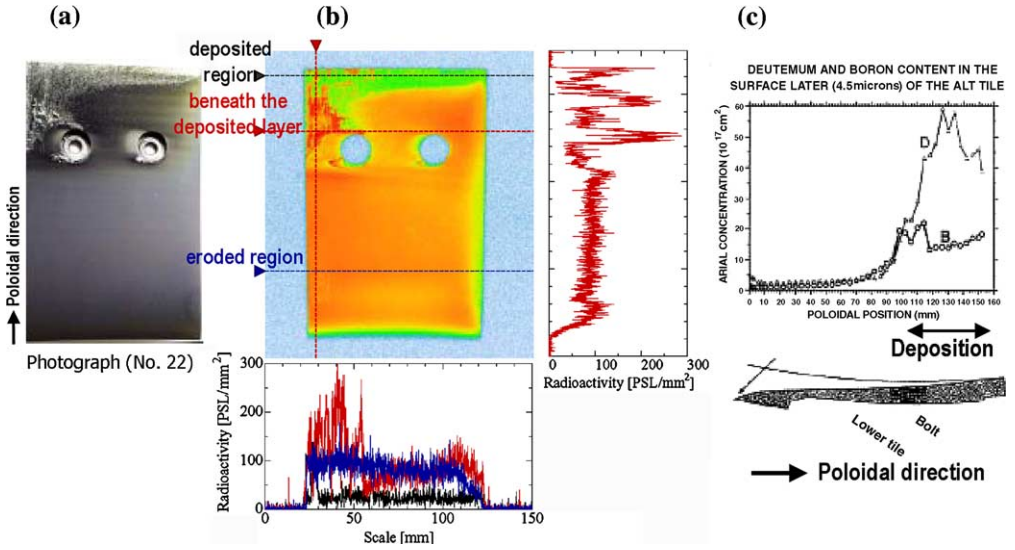


Fig. 6. (a) Photograph, (b) tritium image for a graphite tile (No. 22 at blade 4 of the ALT-II limiter in TEXTOR), together with line profiles along the poloidal (vertical) and toroidal (horizontal) directions [16], and (c) deuterium and boron line profiles along the poloidal direction together with the cross-section of the tile [40]. In the color-coded tritium images, red indicates a higher tritium level while blue indicates the opposite. Vertical and horizontal directions correspond to the poloidal and toroidal directions, respectively, in the torus. Two holes in the central area of the tile are for the bolts fixing the tile to the base plate. The lower and larger part of the tile is the erosion-dominated region, while the upper part with a rough surface is the deposition-dominated region which was covered with re-deposited layers with a thickness of around 5 μm. PSL denotes photo-stimulated luminescence detected by the plate reader and is a measure of surface tritium concentration.

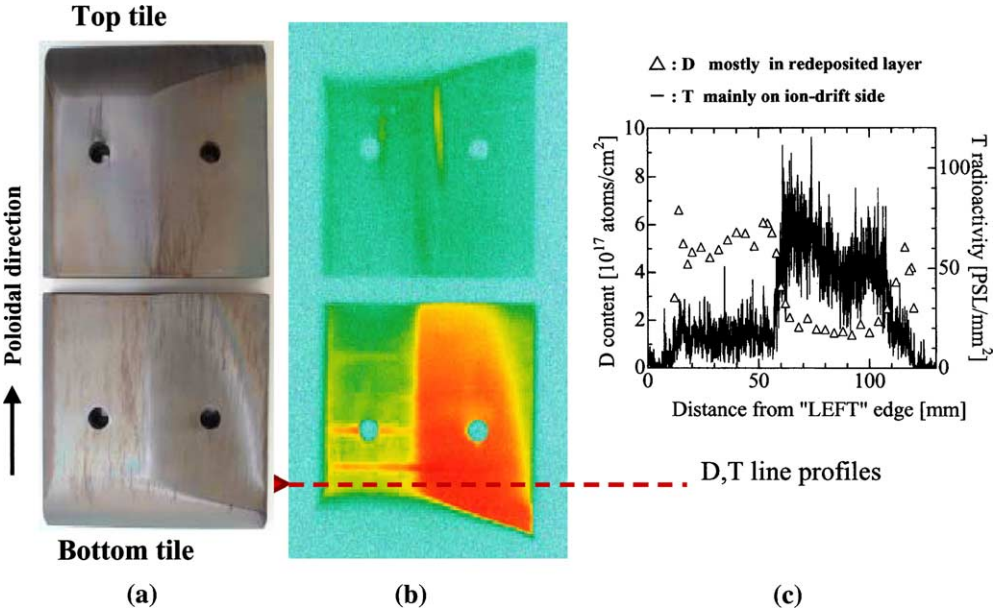


Fig. 7. (a) Photograph, (b) tritium image for graphite bumper limiters (the top and the bottom out of 5 bumper limiters used in TEXTOR, and (c) comparison of deuterium and tritium line profiles along the poloidal direction [16,17]. PSL denotes photo-stimulated luminescence detected by the plate reader and is a measure of surface tritium concentration.

line profiles of deuterium content and the PSL intensity of tritium for the bottom tile are plotted in Fig. 7(c) [17]. Because of the saddle type shape of the tiles, the tritium images may be divided into an electron-drift side (0–60 mm from left edge) and an ion-drift side (60–120 mm from left side). The tritium level is significantly higher for the bottom limiter than for the top one. Similar to the profiles shown in Fig. 6, the profiles for tritium and deuterium as shown in Fig. 7(c) are completely opposite. The appearance of the bumper limiters did not show a clear deposition pattern, but there might be some deposition, as indicated by the observed high retention of deuterium in the electron-drift side (See Fig. 7).

### *4.2. Tritium retention on an inner wall tile from TFTR exposed to D–D discharges*

Fig. 8 compares a photograph, a tritium image and the corresponding PSL intensity line profiles of a tile from the inner limiter of TFTR that had been exposed to D–D discharges only [41]. Unlike the TEXTOR tiles, the tritium distribution on the TFTR tile is quite non-uniform, and little correlation is seen with the deposition patterns which are also non-uniformly distributed on the tile [42]. The reasons may be following. TFTR wall temperatures could exceed 1000 K during a high power discharge, which is also noted as measured D/C ratios of 0–0.2 indicating higher than 400 K temperatures [37]. TFTR experienced a complex balance of wall erosion and deposition on the bumper limiter governed by the magnetic field connection length (see Ref. [38] and references therein). Thus there could be uniform T deposition from the D–D reaction followed by spatially varying erosion, resulting in the non-uniform distribution. To confirm this, further study is needed.

### *4.3. Tritium retention in plasma facing graphite tiles from JT-60U*

The analyzed tiles were exposed to deuterium plasmas in JT60-U in the period from June 1997 to October 1998. During this period, about $10^{19}$ neutrons were generated by D–D reactions, which also produced $10^{19}$ tritium atoms or 18 MBq of tritium [37]. The vacuum vessel was subsequently subjected to hydrogen discharges to remove the tritium retained in the vacuum vessel, then followed by air ventilation before being fully opened to the atmosphere.

Fig. 9 shows tritium images of the divertor units and the baffle plates together with the PSL intensity line profiles corresponding to the red and blue lines in the images [18–20]. As was the case with the TEXTOR tiles, the tritium profiles in the JT-60U tiles did not show a clear correlation with the deposited layers [43]. In JT-60U, deposited layers were found mainly on the inner divertor tiles, though the deposited layer was not clearly distinguished from the substrate [43]. This is probably because the relatively higher temperature during the discharges enhanced the adhesion property of the deposits on the matrix with smaller H and D content than

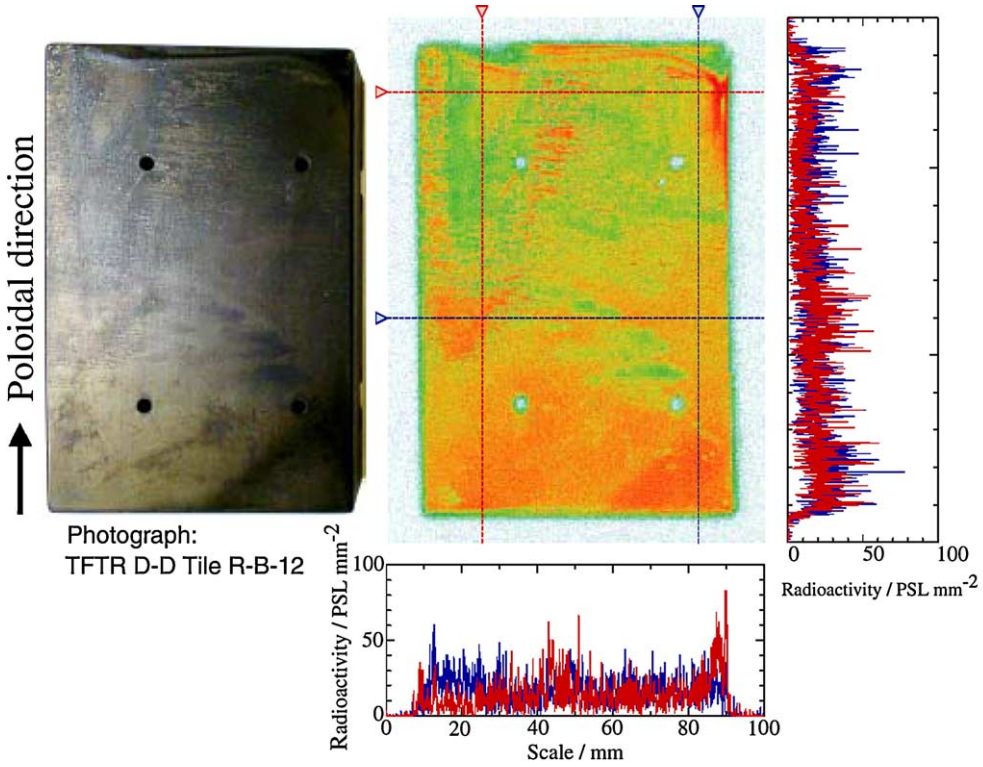


Fig. 8. Comparison of photograph, tritium image for graphite inner wall tiles exposed to D–D discharges in TFTR together with tritium line profiles.

other large tokamaks [34]. The temperature increase of graphite tiles due to the plasma heat load was around 50 K except at the divertor regions where the maximum temperatures of 800 and 1200 K were recorded at the inner and outer divertors, respectively. It was somewhat unexpected to see that the highest tritium level was recorded at the outer baffle plates and the top of the divertor dome, which the plasma did not directly contact. The tritium levels at the top of the dome unit and the baffle plates were estimated to be in the order of 10 kBq/cm$^2$ [19].

The observed tritium distribution in JT-60U divertor tiles can be explained by the implantation of high energy tritium and the simultaneous thermal release due to the heat load [17,18]. Suppose the total produced tritium (18 MBq) in JT-60U was distributed homogeneously over the plasma facing area, one can calculate the surface density of the tritium level to be around 10 kBq/cm$^2$, the same order of the magnitude as the observed tritium level. This suggests that a large part of the tritium produced by D–D reactions was injected uniformly over the plasma facing surfaces and did not fully loose its initial energy of 1 MeV before impinging to the wall [20,21].

The full toroidal tritium distribution on all 240 dome top tiles shown in Fig. 10, also indicates high energy tritium implantation [18]. A periodic variation is apparent with the toroidal angle. In JT-60U, 18 toroidal magnets are placed as indicated in the figure. One can clearly see a similar periodicity in the tritium retention in the toroidal direction. This is the first clear evidence of the loss of high energy tritons by the ripple in the toroidal magnetic field (i.e., 'ripple loss') [18,19].

Furthermore, the tritium profiles of divertor tiles for both cases of inner divertor pumping and both sides pumping show nearly the same tritium distribution. The tritium detected was not influenced by pumping, in other words, there is no significant contribution from gaseous tritium in the tritium distribution of the divertor tiles.

In contrast to the dome top tiles, the tritium level in the divertor tiles were very small. In particular, both the outer and inner strike points showed the lowest level owing to the temperature rise during plasma discharges. One also notes that the tritium level shows a gradient in the poloidal direction. This gradient is inversely correlated to the poloidal temperature distribution, indicating that the implanted tritium was thermally released, resulting in no tritium retention in the divertor legs.

In JT-60U, hydrogen and deuterium depth profiles are also measured for the same divertor tiles used in the tritium analysis. In contrast to TEXTOR, hydrogen and deuterium in JT-60U are distributed quite similarly with tritium, i.e., the area with higher tritium retention also

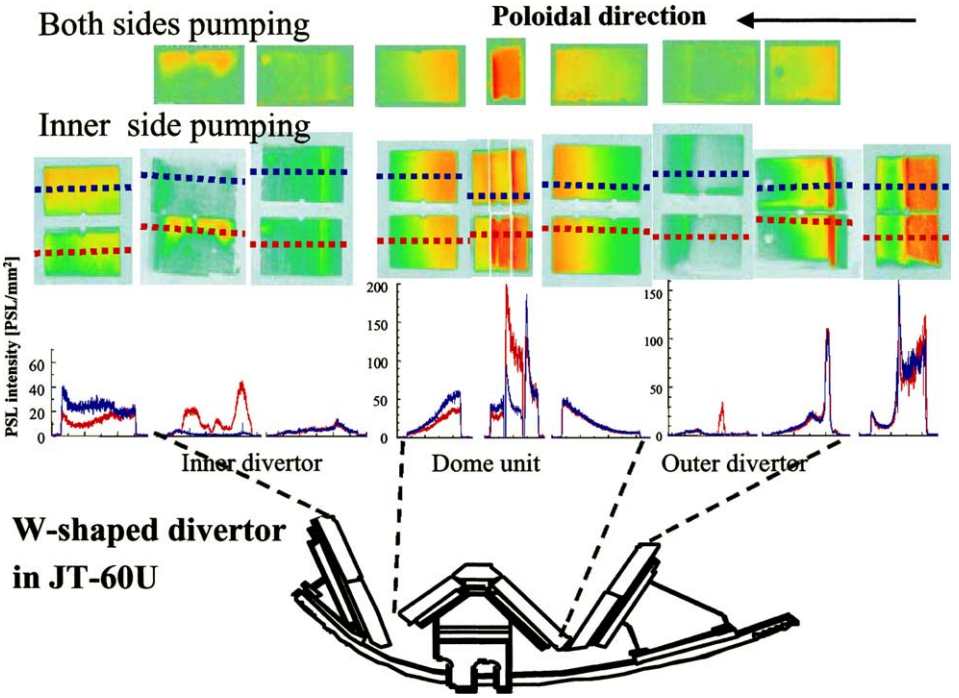


Fig. 9. Tritium distribution on graphite tiles used in JT-60U [18]. (a) Tritium images of divertor tiles used for both sides pumping geometry, (b) those for inner side pumping geometry, and (c) their line profiles along the red and blue lines on the tritium images together with schematic cross-section of divertor area [20].

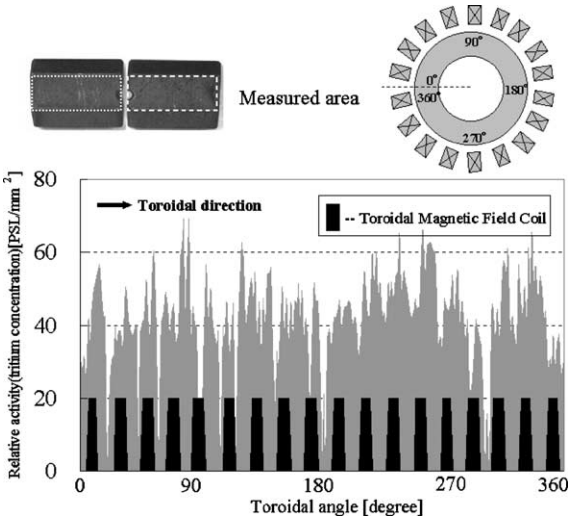


Fig. 10. Full toroidal tritium distribution on the dome top tiles in JT-60U [20].

shows higher hydrogen and deuterium retention [34]. This is another indication that the temperature effect dominated tritium retention in JT-60U.

## 5. Tritium in JET with D–T discharges

Fig. 11 shows the tritium images of JET Mark-II divertor tiles [18]. The numbers in the figure are the tritium levels (in MBq/cm$^2$) determined by combustion method [11–13]. Several characteristic features were observed: (i) as already pointed out the tritium level was the highest in the re-deposited layers particularly in shadowed areas (not directly exposed to the plasma) in the inner divertor, (ii) the inner divertor retains larger amount of tritium, (iii) the divertor tritium distribution in JET is quite different from that in JT-60U and show some patterns in the toroidal direction, (iv) the tritium level is higher at the central area of the inner divertor tiles in the poloidal direction, while the edges retain higher tritium in the outer divertor tiles.

The tritium retention in the deposited layer is confirmed by the measurements of exfoliated area as indicated in Fig. 12 [22]. On the JET tile, the re-deposited layers were easily exfoliated by an adhesive tape. The tritium image for the exfoliated region and the backside of the exfoliated film are given in Fig. 12. From the line profile of the PSL intensity including the exfoliated layer, one can note that most of the tritium is retained in the re-deposited layers. However the tritium level of the backside of the exfoliated layer is about one half of that

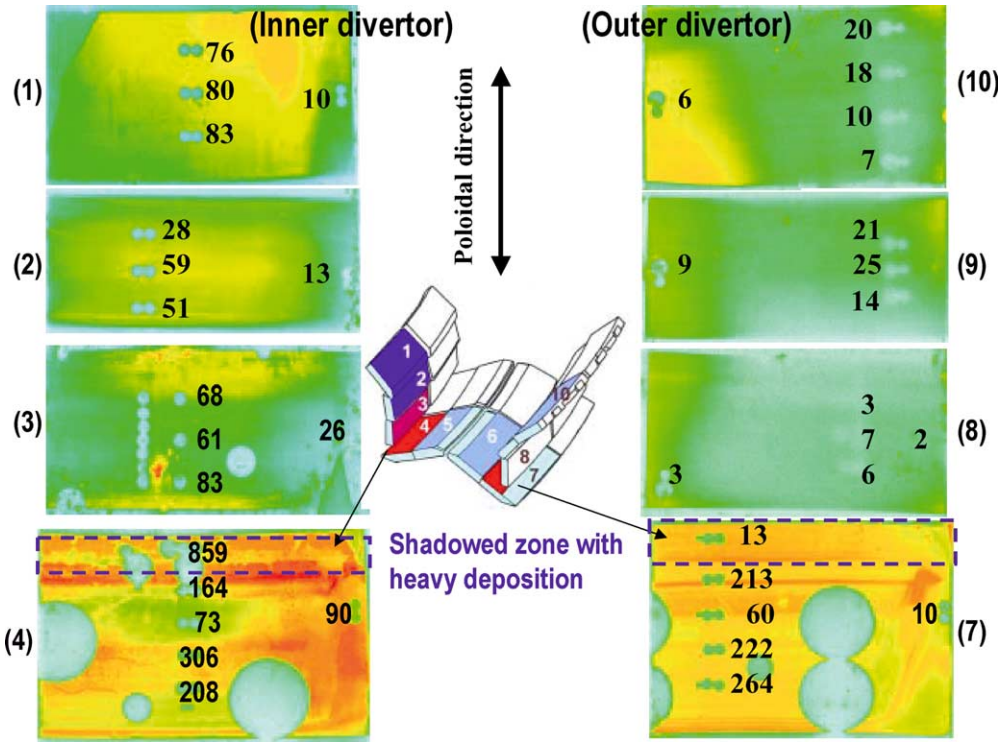


Fig. 11. Tritium image for whole divertor area in JT-60U [22]. The numbers in the image are the tritium surface concentration within 1 mm from the surface measured by the coring/combustion technique in MBq/cm$^2$ [1,3].

on the top surface. This indicates again that most of the tritium is retained in the front surface region of the re-deposited layers (see also Ref. [11]). It should also be noted that the tritium level beneath the deposited layers was much less (more than one order of magnitude) than that of the re-deposited layer and very similar to that for the plasma facing central area.

In JET, the divertor base (the supporting structure) is water cooled and the base temperature of the divertor tiles was reported to be around 500 K, cooler than the ambient temperature of the rest of the torus (600 K) [4]. Therefore tritium from the plasma (including both the high energy tritium and the edge plasma tritium) was retained without significant changes in their profiles (the former was implanted into the subsurface and the latter co-deposited with carbon) [22,44]. As observed in Fig. 6, however, the tritium images for the outer and the inner divertors were quite different. This is mainly owing to the fact that the outer divertor area is erosion dominated, while the inner divertor deposition dominated. Accordingly, the tritium on the outer divertor could be dominated by the high energy tritium, whereas the co- or re-deposited tritium dominates on the inner divertor.

Another difference between the inner and outer divertor tiles appears in the toroidal non-uniform patterns. Such toroidal non-uniformity was not appreciable in JT-60U (see Fig. 9). The non-uniformity in JET could be attributed to erosion-deposition pattern. The tiles were slightly curved to the appropriate radius to have homogeneous heat load. Even so, about 3 cm of one toroidal end is always in the shadow of the upfield tile. This is likely the main reason for the higher tritium measurement by the IP technique at the edge of the outer divertor tiles.

However, one can clearly see the discrepancy between the IP measurements and the combustion measurements for the outer divertor tiles (tiles #8–#10 in Fig. 11), i.e. the IP measurements show higher tritium corresponding the deposition discussed above, whereas the combustion measurements show the opposite. In addition the tritium level of the outer divertor tiles are significantly less than that for the inner divertor tiles, particularly the tile #8 retained quite a small amount. This may suggest thermal release. As shown in Fig. 3, if the surface temperature rose above 500 K, the temperature effect could be dominant. The toroidal length of JET divertor tiles is long enough that the plasma heat load or particle flux may not be homogeneous. This could result in a higher flux or a higher temperature in the central area compared to the edge. Similarly the edge region on the inner divertor must also experience a higher heat load, resulting in a higher temperature compared to the center.

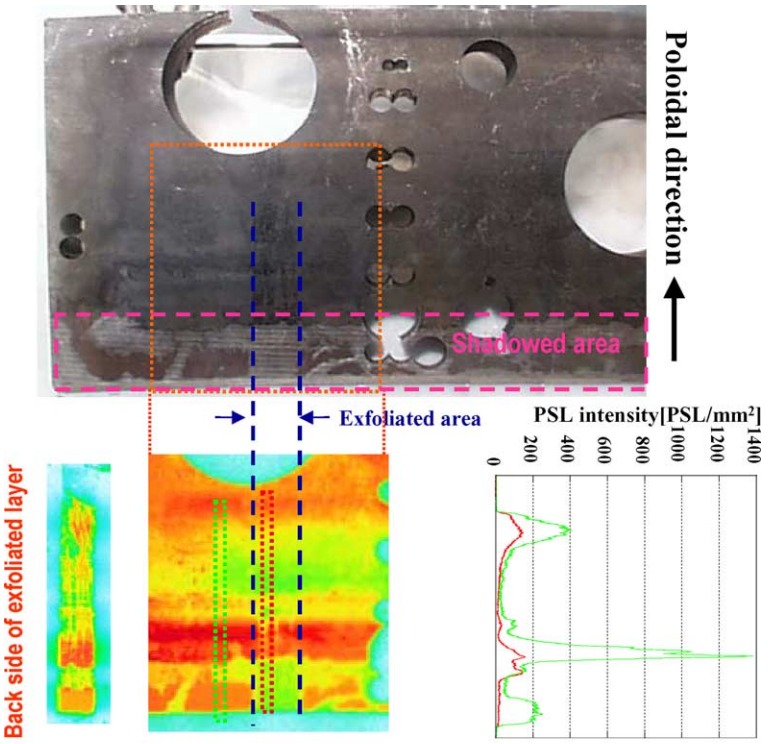


Fig. 12. Tritium profiling beneath the exfoliated area deposits and the back side of the exfoliated layers on the inner divertor target tile BN4 in JET [22].

Consequently, tritium level is observed to be lower in the central area compared to the edge region at the outer divertor and vice-versa at the inner divertor. More investigation is needed on the temperature effect on JET. One must also bear in mind that the IP technique is sensitive only to tritium in the top few microns of the surface region and this could have been influenced by the extensive clean up campaign before tile removal from JET.

## 6. Discussion on tritium retention in a D–T reactor

As discussed in Section 2, one may distinguish three different tritium species in a fusion reactor, i.e. high energy tritium, edge plasma tritium, and gaseous tritium. In this section, the roles of the three components in tritium retention of D–T reactors are summarized based on the above observations.

### 6.1. High energy tritium

In TEXTOR [15–17] and JT-60U [18–21], the retention mechanism of tritium in D–D discharge machines is via high energy tritium implantation, i.e. a large part of triton produced by the D–D reaction is implanted into the walls without being fully thermalized in the plasma. Even in JET tiles, we can see indications of this type of tritium injection mechanism from the following observations; (i) similar tritium level on all the outer divertor tiles (in the order of MBq/cm$^2$ orders), (ii) similar tritium level beneath the exfoliated layers and the smallest level on the inner divertor tiles (i.e., in the erosion dominated regions). Since this tritium level (in the order of MBq/cm$^2$) is three orders of magnitude smaller than that that in the re-deposited layer (in the order of GBq/cm$^2$), the total specific tritium level may be much smaller, but the high energy tritium is implanted in all plasma facing component within a specific depth. In addition, the tritium implanted in specific depth with low concentration might not be easily removed compared to tritium in the co-deposited layers where hydrogen is saturated. Although the high energy tritium must be well confined in D–T reactors, it could be a serious concern [1,2].

The top and bottom asymmetry observed in the bumper limiters of TEXTOR seems to reflect the character of plasma or the gyration of energetic particles, showing higher tritium deposition on the bottom than on the top [16,17]. Thus the examination of the high energy tritium profiles could be a new diagnostic for the behavior of high energy tritons in a plasma.

### 6.2. Edge plasma tritium

The main source of tritium inventory in JET seems to be co-deposition that appeared mostly in the shadowed area not exposed directly to the plasma, with a large amounts of tritium being retained. However, if we could maintain the temperature of most of the surface area above 700 K as observed in divertors in JT-60U, the tritium inventory by the co-deposition mechanism could be significantly reduced.

### 6.3. Gaseous tritium

The gaseous tritium can be absorbed at any location in the torus as observed in the rear side surface of the JET tiles (see Fig. 13). One can see that preferential absorption and migration of gaseous tritium into the CFC tile likely the cause of the striped tritium image in the 2-D CFC tiles. This is because the fibers and the matrix are differently graphitized in 2-D CFC and absorption characteristics to the gaseous hydrogen may be different between the successive layers [16]. The depth profiles of the tritium both by the combustion and by the IP technique clearly show migration of tritium deep inside indicating tritium penetration along the boundary between the fibers and matrix, whereas the backside surface showed a slightly higher tritium level, indicating the absorption from the back side [11,22]. The actual tritium level retained by the absorption mechanism is very small compared to the co-deposition mechanism. However, the absorption occurs everywhere (even in surfaces of pores in the graphite bulk as appeared in the stripe pattern in Fig. 13) and the integrated amount could be significant. To reduce this inventory, a higher temperature (over 1200 K) is needed and this inventory could dominate in a D–T power reactor with carbon plasma facing components (if carbon is used). Since the tritium concentration by gaseous tritium uptake is very small compared to the implantation and to the co-deposition, one may need a higher desorption temperature to remove this, as already discussed in Section 2.

### 6.4. Effect of temperature on tritium inventory

Tritium retention in the JT-60U tiles is not strongly correlated with the re-deposition patterns and the highest tritium level was observed at the top of the dome and on the divertor baffle plates where they were directly exposed to the plasma (situated very near the plasma and not shadowed). Tritium distribution was strongly modified by surface temperature: no tritium was detected on both divertor legs, and gradual profile changes along the poloidal direction have an inverse tendency to the temperature profile. Again H and D profiles were very similar indicating a temperature controlled retention mechanism.

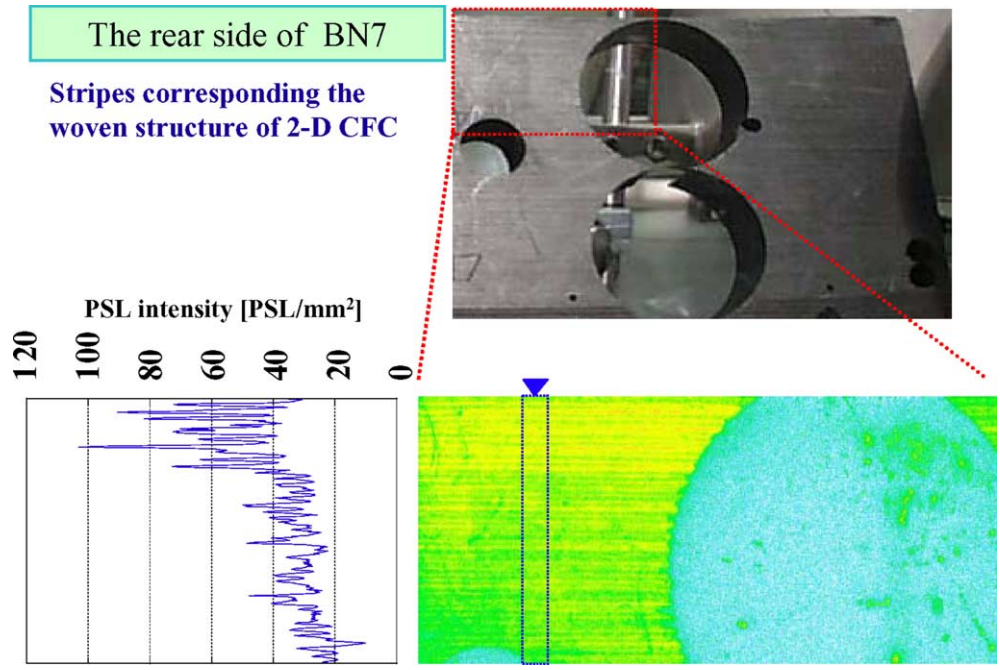


Fig. 13. Tritium image and line profile for the rear side surface of BN7 in JET [22]. One can clearly see stripes in the tritium image and the periodic intensity change in the line profile, which is just the same as the woven layered structure of the two dimensional CFC tile used as a divertor tile.

In this respect, retained hydrogen (including all isotopes) H/C ratio could be a good indirect measure for the tile temperature. For example, referring to Fig. 3 [30,45], the observed D/C ratio of ~0.05 in the bumper limiter in TEXTOR [40] (see Fig. 7) indicates that the limiter temperature must have reached above 900 K. The asymmetry in the deuterium retention between the electron side and the ion side of the bumper limiters might also be attributed to temperature differences. In JET tiles, not only an inner–outer asymmetry was significant but also there was a non-uniform toroidal distribution along a tile. These profiles are most probably due to shadowing, but heat load asymmetry could also result in such profiles.

In order to reduce tritium in vessel inventory in a D–T reactor, maintaining all plasma facing temperatures above 1000 K during plasma shots seems beneficial. This might have occurred in the neighborhood of the divertor legs of JT-60U, where the temperature before discharge was around 600 K and rose easily above 800 K, resulting in a very small hydrogen (including H, D, T) retention.

## 7. Summary and conclusions

The tritium retention in large tokamaks, all of which use carbon plasma facing components, is investigated and the results interpreted according to the present knowledge for hydrogen–carbon chemistry.

Tritium impinging on the vessel wall has three different components; high energy tritons escaping from the main plasma, edge plasma tritium from the boundary plasma, and the gaseous tritium. The high energy tritons are likely implanted into all plasma facing surfaces relatively deeply and homogeneously with a maximum implanted depth of several micrometers. It is found that the observed tritium distribution clearly shows symmetries in poloidal and toroidal directions. The toroidal tritium distribution in JT-60U clearly shows the ripple loss due to toroidal field inhomogeneity. The edge plasma tritium is mostly co-deposited onto shadowed areas with low surface temperatures. This is the main tritium retention mechanism in JET. A very small fraction of the gaseous tritium is absorbed everywhere, even on surfaces of inner pores of graphite bulk owing to its porous nature.

The temperature dependence of tritium retention by these three components is different because they are retained at different depths with different concentrations. The high energy tritium is implanted deeply and more uniformly distributed all over the first wall surfaces than the highly localized co-deposited tritium from the edge plasma near the divetor region. The long term inventory could be reduced if the surface temperature is higher. If we could maintain the temperature of the deposited area above 1000 K, tritium inventory may be reduced significantly.

In the present tokamaks, the contribution of the gaseous tritium is far smaller than the other two, although the inventory caused by the gaseous tritium may remain as the hardest inventory to be removed, because mostly backside and/or shadowed area from the plasma contribute to this inventory. Taking these all into account, we propose maintaining the plasma facing surface temperature at about 1000 K during plasma shots in order to reduce the tritium inventory in carbon based plasma facing components of a D–T reactor.

## Acknowledgements

This work has been partly supported by a Grant-in-Aid for scientific research by the Ministry of Education, Culture, Sports, Science and Technology of Japan and partly performed within the Tritium Laboratory Karlsruhe (TLK) under the framework of the program Nuclear Fusion of the Forschungszentrum Karlsruhe. The support of the European Commission under the European Fusion Development Agreement (EFDA) is also gratefully acknowledged.

## References

[1] G. Federici, R.A. Anderl, P. Andrew, et al., J. Nucl. Mater. 266–269 (1999) 14.
[2] G. Federici, C.H. Skinner, J.N. Brooks, et al., Nucl. Fusion 41 (2001) 1967.
[3] R.A. Causey, J. Nucl. Mater. 300 (2002) 91.
[4] P. Andrew, P.D. Brennan, J.P. Coad, et al., Fusion Eng. Des. 47 (1999) 233.
[5] C.H. Skinner, J.T. Hogan, J.N. Brooks, et al., J. Nucl. Mater. 266–269 (1999) 940.
[6] C.H. Skinner, C.A. Gentile, K.M. Young, J.P. Coad, J.T. Hogan, R.-D. Penzhorn, 28th EPS Conference on Controlled Fusion and Plasma Physics Madeira, Portugal, 18–22 June 2001, http://www.cfn.ist.utl.pt/EPS2001/fin/pdf/P4.080.pdf. Europhys. Conf. Abs. 25A (2001) 1621.
[7] G. Federici, J.N. Brooks, M. Iseli, C.H. Wu, Phys. Scr. T91 (2001) 76.
[8] G. Federici, J.N. Brooks, D.P. Coster, et al., J. Nucl. Mater. 290–293 (2001) 260.
[9] G. Federici et al., these Proceedings. PII: S0022-3115(02)01327-2.
[10] C.H. Skinner et al., these Proceedings. PII: S0022-3115(02)01382-X.
[11] R.-D. Penzhorn, J.P. Coad, N. Bekris, L. Doerr, M. Friedrich, W. Pilz, Fusion Eng. Des. 56&57 (2001) 105.
[12] R.D. Penzhorn, N. Bekris, U. Berdnt, et al., J. Nucl. Mater. 288 (2001) 170.
[13] R.D. Penzhorn, N. Bekris, P. Coad, et al., Fusion Eng. Des. 49&50 (2000) 753.
[14] C.H. Skinner, C.A. Gentile, G. Ascione, et al., J. Nucl. Mater. 290–293 (2001) 486.
[15] T. Tanabe, V. Philipps, Fusion Eng. Des. 54 (2001) 147.

[16] K. Miyasaka, T. Tanabe, G. Mank, et al., J. Nucl. Mater. 290–293 (2001) 448.
[17] T. Tanabe, K. Miyasaka, M. Rubel, V. Philipps, Fusion Sci. Technol. 41 (2001) 924.
[18] K. Miyasaka, T. Tanabe, K. Masaki, N. Miya, Proc. ICFRM-10, J. Nucl. Mater., in press.
[19] T. Tanabe, K. Miyasaka, K. Sugiyama, K. Masaki, K. Kodama, N. Miya, Fusion Sci. Technol. 41 (2002) 877.
[20] K. Sugiyama, T. Tanabe, K. Masaki, K. Kodama, N. Miya, International Workshop on Hydrogen Isotopes in Fusion Reactor Materials, 22–26 May 2002, Tokyo, Japan, Phys. Scr., in press.
[21] K. Masaki, K. Sugiyama, T. Tanabe, Y. Gotoh, K. Miyasaka, K. Tobita, Y. Miyo, K. Kaminaga, K. Kodama, T. Arai, N. Miya, Tritium Distribution in JT-60U W-shaped Divertor, these Proceedings. PII: S0022-3115(02)01388-0.
[22] K. Sugiyama, K. Miyasaka, T. Tanabe, M. Glugla, N. Bekris, Tritium distribution on the surface of plasma facing carbon tiles used in JET, these Proceedings. PII: S0022-3115(02)01387-9.
[23] W. Jacob, W. Möller, Appl. Phys. Lett. 63 (1993) 1771.
[24] R.A. Causey, J. Nucl. Mater. 162–164 (1989) 151.
[25] K.L. Wilson et al., Suppl. J. Nucl. Fusion 1 (1991) 31.
[26] M. Jacob, W. Möller, Appl. Phys. Lett. 63 (1993) 1771.
[27] W.O. Hoffer, J. Roth, Physical Process of the Interaction of Fusion Plasma with Solids, Academic Press, 1996.
[28] W. Jacob, Thin Solid Films 326 (1998) 1.
[29] T. Tanabe, S. Muto, Phys. Scr. T 81 (1999) 104.
[30] B.L. Doyle, W.R. Wampler, D.K. Brice, J. Nucl. Mater. 103&104 (1981) 513.
[31] H. Atsumi, M. Iseki, T. Shikama, J. Nucl. Mater. 212–215 (1994) 1478.
[32] D.P. Stotler, C.H. Skinner, R.V. Budny, A.T. Ramsey, D.N. Ruzic, R.B. Turcot, Phys. Plasmas 3 (1996) 4084.
[33] K. Tobita, S. Nishio, S. Konishi, et al., Fusion Eng. Des., in press.
[34] Y. Hirohata, Y. Oya, H. Yoshida, et al., International Workshop on Hydrogen Isotopes in Fusion Reactor Materials, 22–26 May 2002, Tokyo, Japan, Phys. Scr., in press.
[35] T. Tanabe, H. Atsumi, J. Nucl. Mater. 209 (1994) 109.
[36] M.A. Pick, H. Altmann, D. Ciric, E.B. Deksnis, H.D. Falter, J. Fantohome, C. Lowry, P. Massman, R.B. Mohanti, A.T. Peacock, R.B. Tivery, J. Nucl. Mater. 220–222 (1995) 473.
[37] K. Masaki, K. Kodama, et al., Fusion Eng. Des. 31 (1996) 181.
[38] C.H. Skinner, W. Blanchard, N.J. Brooks, J. Hogan, J. Hosea, D. Mueller, A. Nagy, Proceedings of the 20th Symposium on Fusion Technology, Marseille, 7–11 September 1998, vol. 1, p. 153; Association EURATOM-CEA, Cadarache, France, September 1998.
[39] M. Matsuyama, T. Tanabe, N. Noda, et al., J. Nucl. Mater. 290–293 (2001) 437.
[40] M. Rubel, J. von Seggern, et al., J. Nucl. Mater. 266–269 (1999) 1185.
[41] W.R. Wampler et al., J. Vac. Sci. Technol. A 6 (1988) 2111.
[42] T.Q. Hua, J.N. Brooks, J. Nucl. Mater. 196–198 (1992) 514.
[43] Y. Gotoh, J. Yagyu, K. Kizu, K. Masaki, K. Kaminaga, K. Kodama, T. Arai, T. Tanabe, N. Miya, Analyses of Erosion and Re-deposition Layers on Graphite Tiles Used in the W-shaped Divertor Region of JT-60U, these Proceedings.
[44] C. Stan-Sion, R. Behrish, J.P. Coad, et al., J. Nucl. Mater. 290–293 (2001) 491.
[45] D.K. Brice, Nucl. Instrum. and Meth. B 44 (1990) 302.